

# NOVEL OPTICAL FIBERS AND SENSORS FOR DIODE LASER SPECTROSCOPY IN NEAR- AND MID-INFRARED REGIONS

**M.I.Belovolov**

*Fiber Optics Research Center of the Russian Academy of Sciences,  
38 Vavilov st., 119333, Moscow, Russia  
E-mail: [bmi@fo.gpi.ru](mailto:bmi@fo.gpi.ru)*

## Content

### 1. Introduction

### 2. New fibers

2.1. Microstructured fibers with very large mode field area ( $\varnothing \sim 100 \mu\text{m}$ )

2.2. Hollow-core PCF fibers with large MFA (fiber cells)

2.3. New silica negative curvature hollow core fiber (NCHCF) for spectral range  $2,5 \div 8 \mu\text{m}$

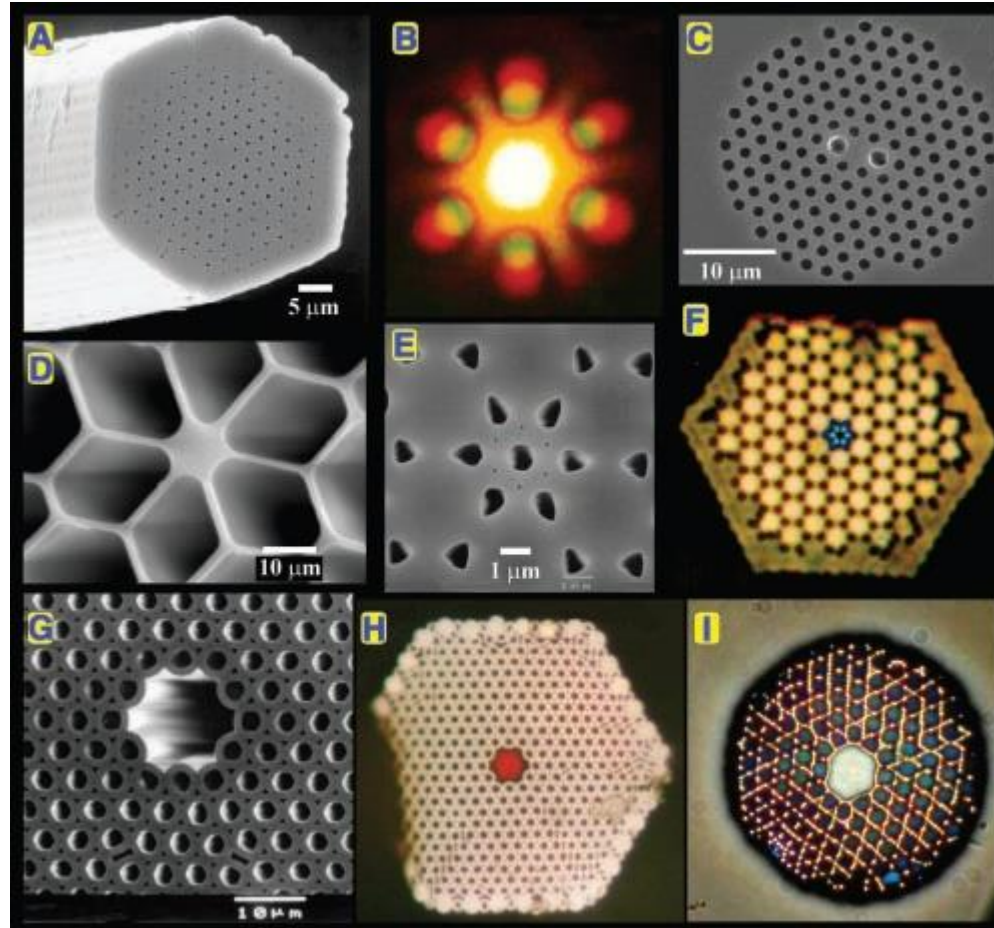
### 3. New lasers for TDLS

3.1. Bismuth-doped glasses, fibers, lasers and amplifiers for  $1000 \div 17000 \mu\text{m}$

3.2. Broad tunable (~ 40 nm) single-frequency DFB-fiber lasers

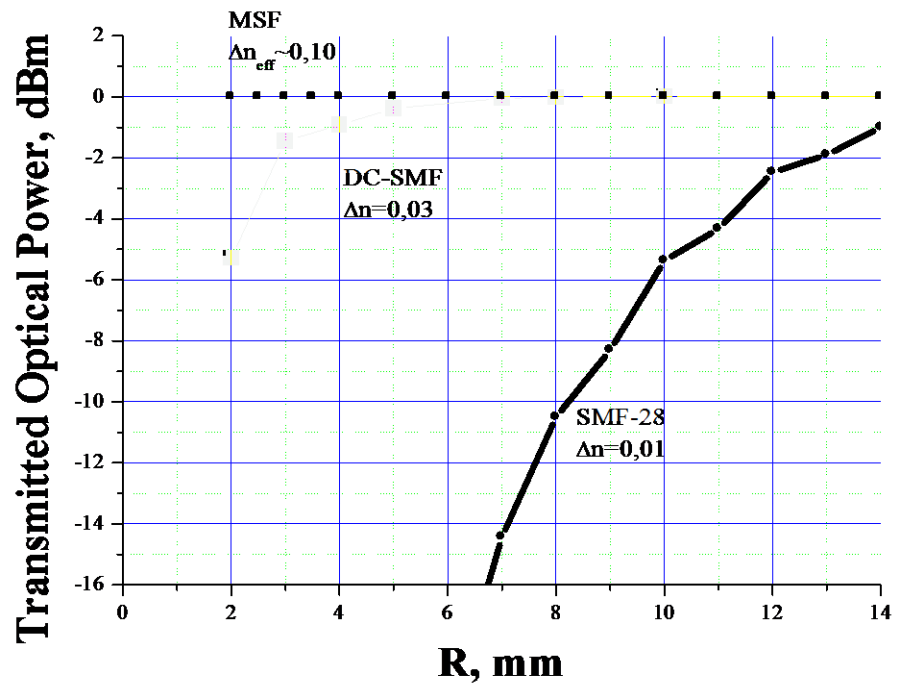
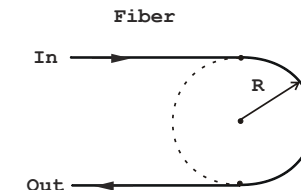
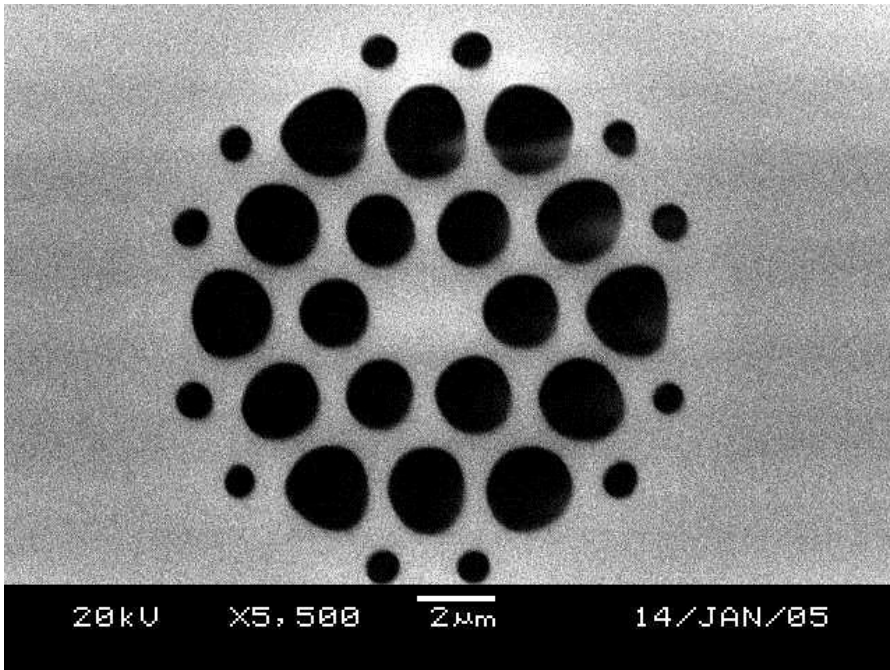
### 4. Conclusion

## Microstructured fibers

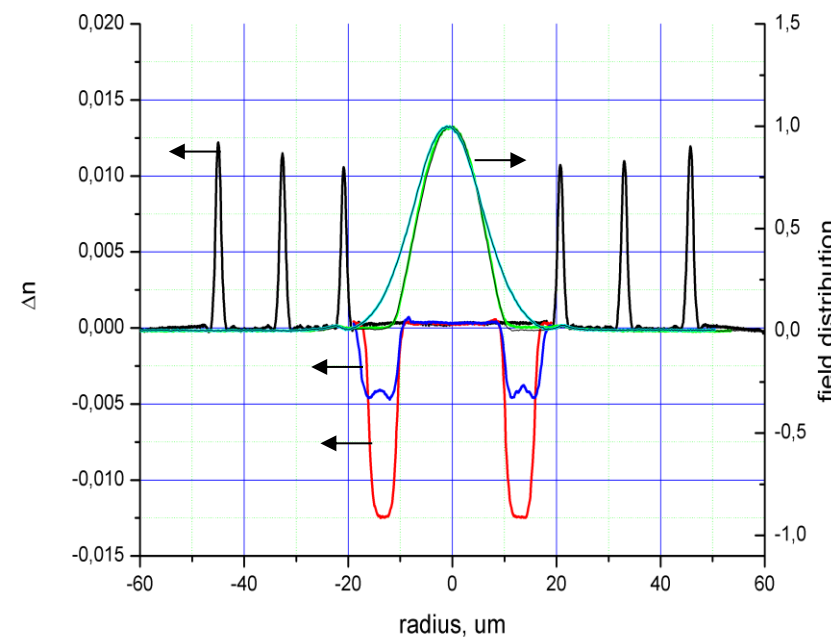
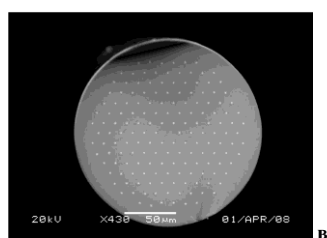
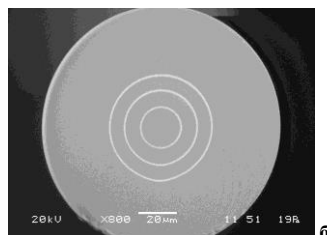
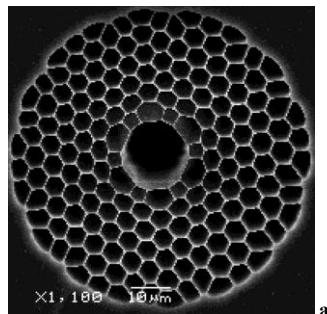


## 2. New fibers

**Microstructured fibers for sensing applications**  
*(small bending radius, small mode field diameter)*



- Microstructured Bragg fibers with large mode field area ( $\varnothing \sim 40 \mu\text{m}$ )



# Microstructured fibers with very large mode field diameter $\varnothing 105 \mu\text{m}$ ( MFA ~ 8600 $\mu\text{m}^2$ )

Tino Eidam, Jan Rothhard et.al., *Fiber chirped-pulse amplification system emitting 3.8 GW peak power.* – *Optics Express, Vol.19, No 1, 2011, pp.255 – 260.*

An Ytterbium-doped large-pitch fiber with a mode field diameter of **105  $\mu\text{m}$**  as the main amplifier was used.

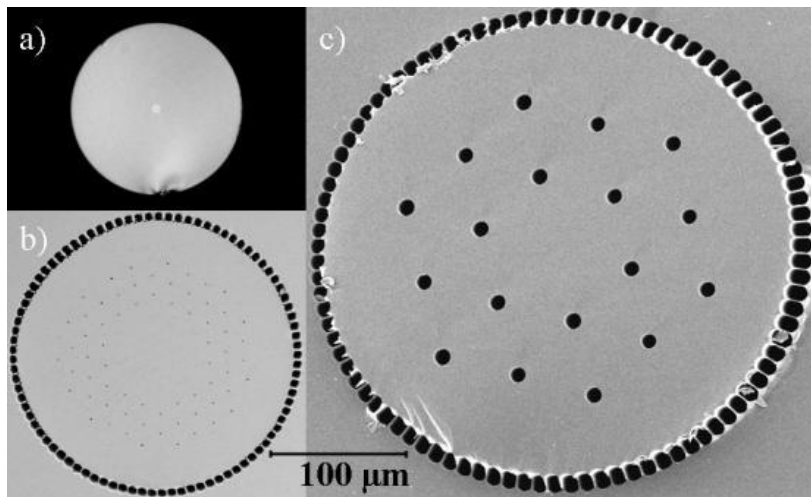


Fig. 1. Microscope images (all at the same scale) of a) standard step index fiber with 6  $\mu\text{m}$  core and 125  $\mu\text{m}$  outer diameter, b) 85  $\mu\text{m}$  core rod type LPF with 200  $\mu\text{m}$  airclad diameter, and c) 108  $\mu\text{m}$  core LPF with 340  $\mu\text{m}$  airclad diameter.

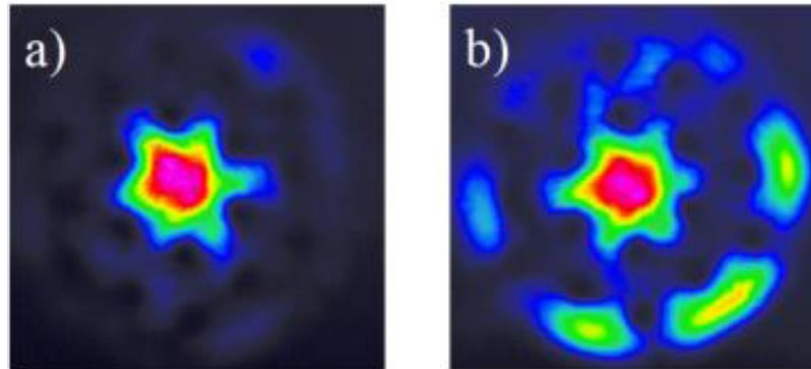


Fig. 3. Near field images of the LPF output beam profile for a) low output powers and b) for the maximum power level. Signal energy contained in the outer ring of the pump cladding is cut in the compressor (and therefore not included in the power measurements) and also blocked for M2 measurements.

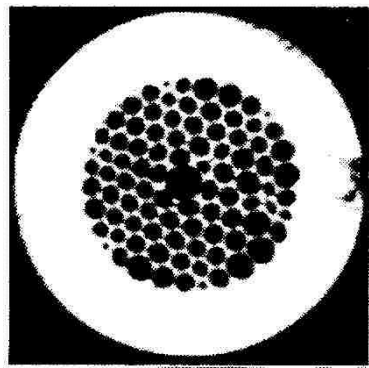
# Microstructured fibers

## SOLID CORE PCF GAS SENSOR

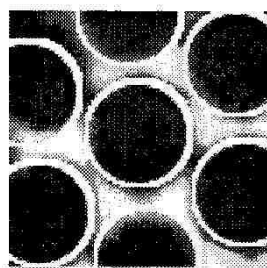
H.Lehmann, S.Bruckner, J.Kobelke, G.Schwotzer, K.Schuster, R.Willsch.

**Toward photonic crystal fiber based distributed chemosensor.**

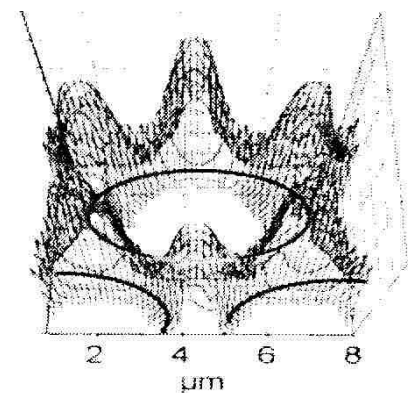
– 17-th Int. Conf. on Optical Fiber Sensors, Bruges, Belgium, 2005; Proc. SPIE Vol. 5855, 419 – 422 (2005).



a) PCF micrograph



b) calculated honeycomb lattice pattern



c) field distribution around a cladding hole

Fig. 5: Field calculation for an isolated hole in the cladding structure of a hollow core fiber.

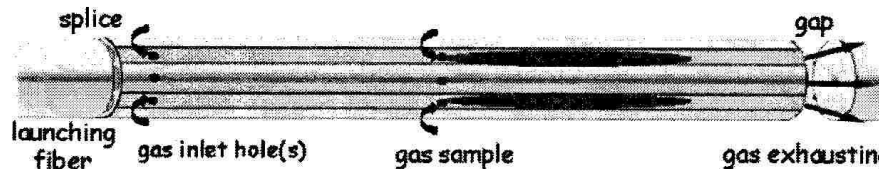
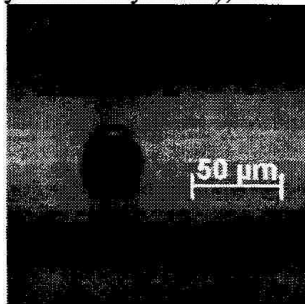
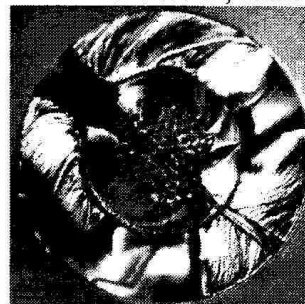


Fig. 6 PCF based quasi-distributed gas sensor (schematically)

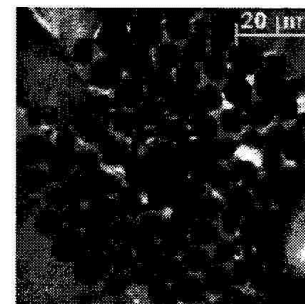
Considering the small diameter of fiber and the brittleness of the fragile PC-structure, the application of gas inlet holes may appear by laser drilling only. Laser drilling attempts on PCF has been performed to several fiber samples using an F-laser (193 nm) with a repetition rate of 50 Hz. The aperture of the laser was masked with a pinhole of 0.4 mm diameter. Fig. 8 shows an example of a laser-drilled radial hole in a hollow core fiber cladded with PDMS (polydimethoxsilane), drilled with  $10^3$  laser pulses of  $1.98 \text{ J/cm}^2$ , each.



a) cladding view



b) fiber cross section



c) capillary structure cross section

Fig. 7: Laser-drilled hole through a hollow-core PCF structure

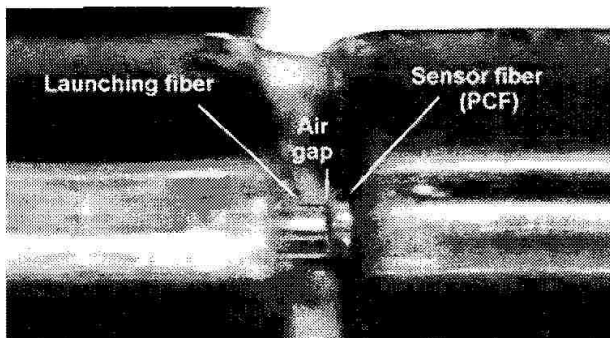


Fig. 3: Fiber/fiber coupling between PCF and launching fiber

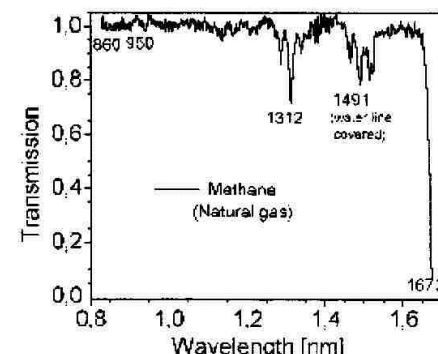


Fig. 4: Methane spectrum, measured by a 1.8 m PCF gas sensor

# Gas sensing with suspended core fibers and hollow core band-gap fibers – a comparative study

H.Lehmann, J.Kobelke et.all., 20<sup>th</sup> Int. Conf. on Optical Fiber Sensors, Proc. of SPIE Vol.7503, 75035C.

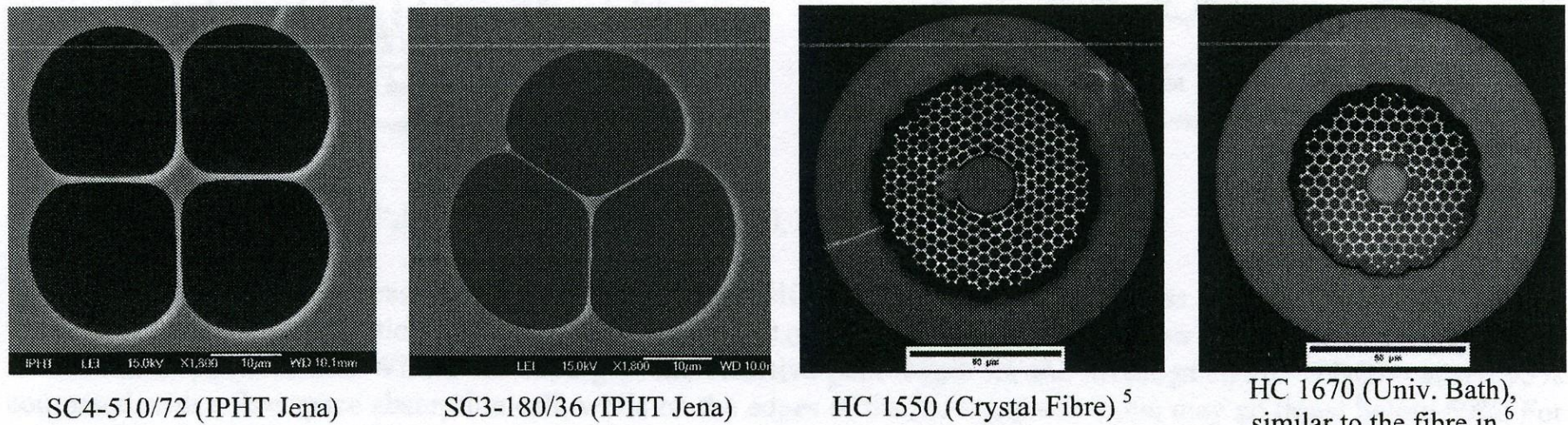


Fig.1: Investigated fibers

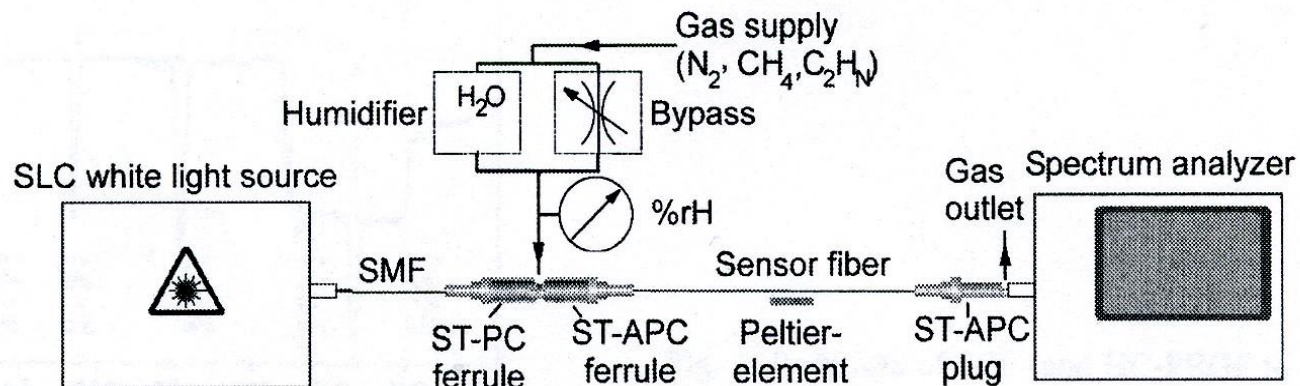


Fig.2: Experimental setup

## Experimental results

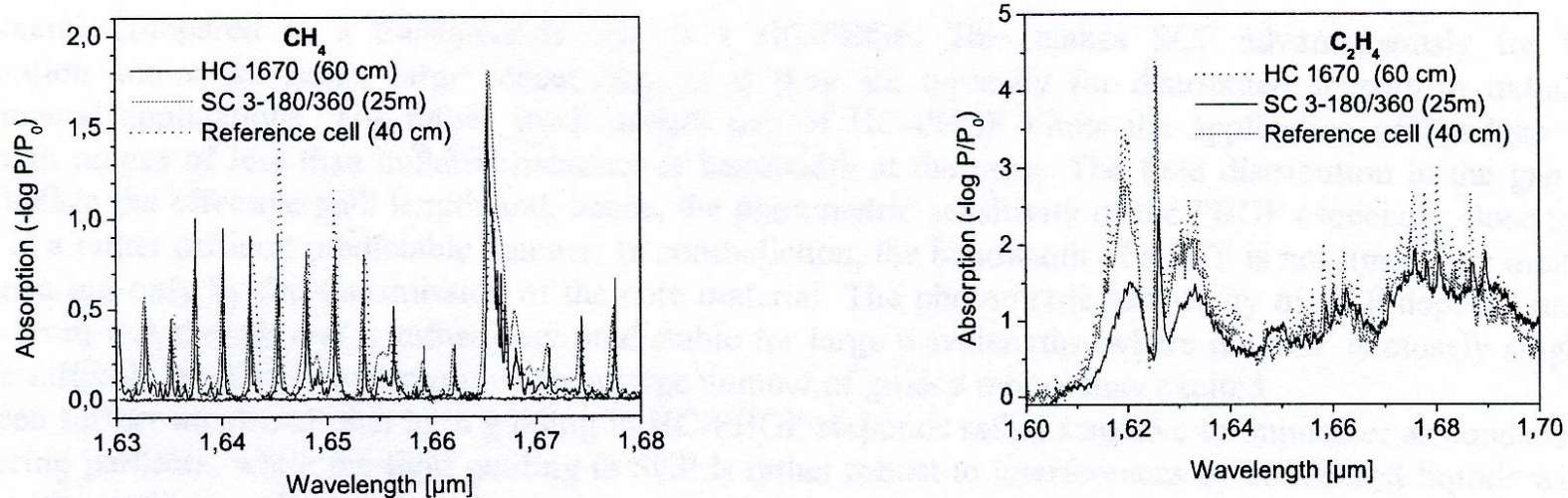


Fig. 3: Gas spectra of  $\text{CH}_4$  and  $\text{C}_2\text{H}_4$  obtained by the reference cell, HC-PBGF and SCF

## **Conclusions**

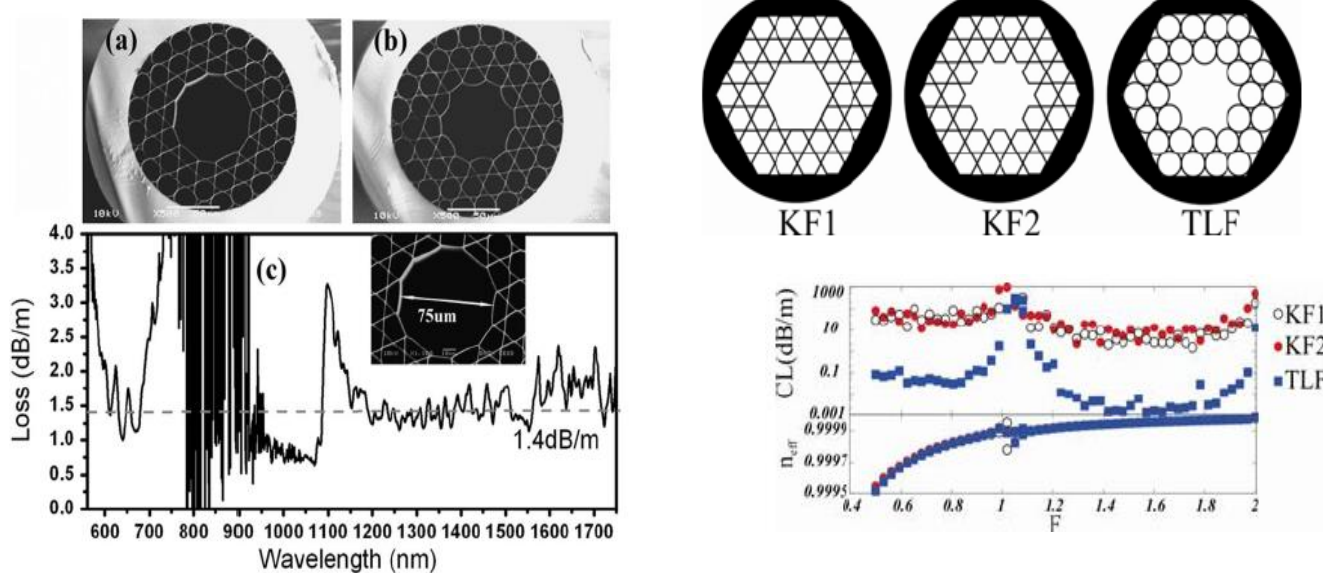
**It has been found that the HC-PBGF may be considered closely as a conventional cell, make them useful especially to detect very small gas concentrations with optical path length up to some meters.**

**For gas sensing HC-PBGF may be most favourable for trace gas analysis in rather clean gas mixtures, while SCF may find their place in rather rugged, distributed sensor for long distances and/or rather high gas concentrations.**

# Negative curvature hollow core fibers - NCHCF

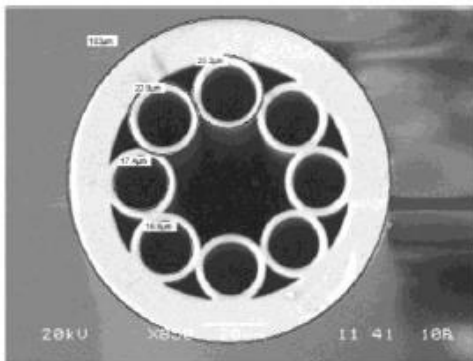
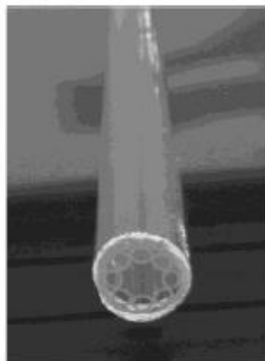
## Полые световоды с дискретной симметрией границы сердцевина – оболочка (negative curvature hollow core fibers)

Y. Y. Wang, N. V. Wheeler, F. County, P. J. Roberts, and F. Benabid, Optics Letters, v. 36, p. 669 (2011) L. Vincetti, V. Setti, and M. Zoboli, SOF'2011, SOWB3

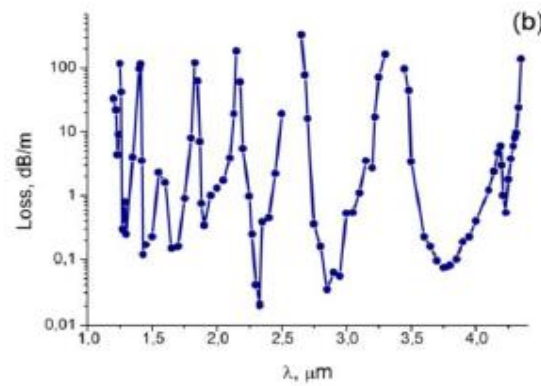
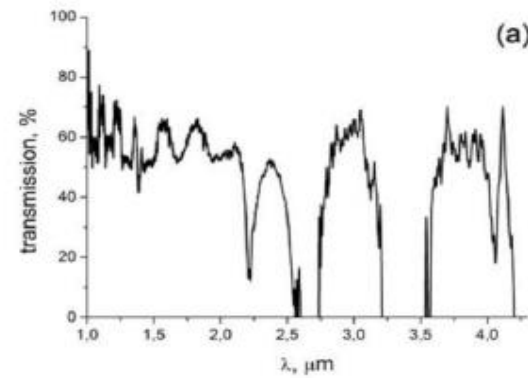


# NCHCF – Negative curvature hollow core fiber for spectral range 2.5 – 8 $\mu\text{m}$

## Оптические свойства полых с дискретной симметрией сердцевина - оболочка

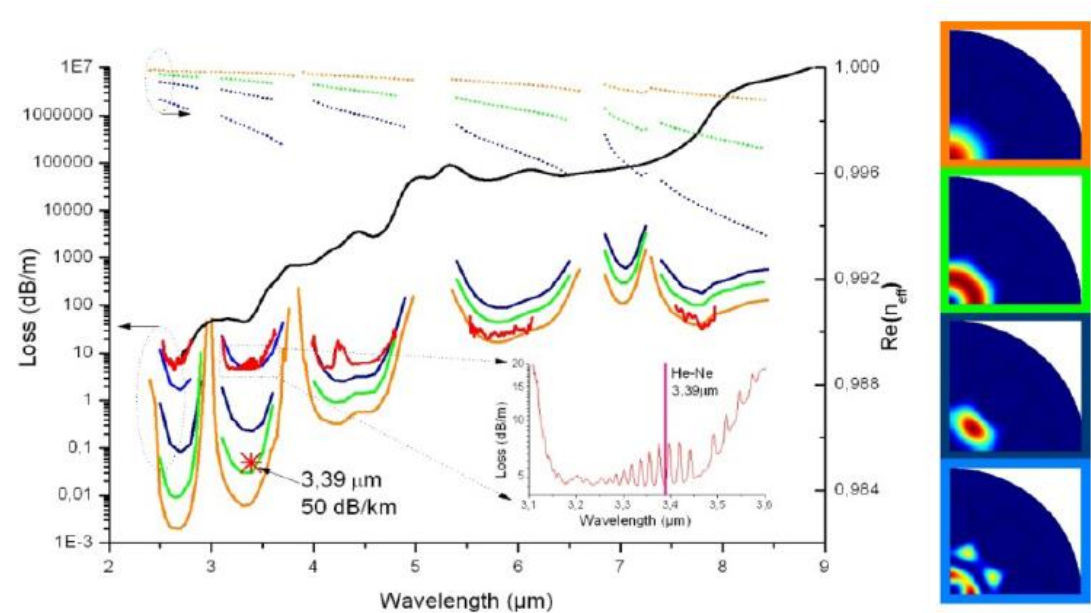
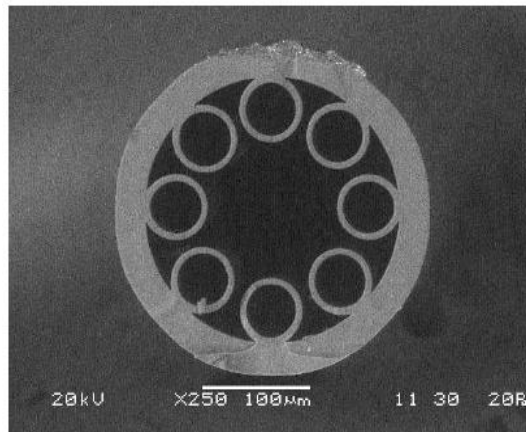


A. D. Pryamikov, A. S. Biriukov, A. F. Kosolapov,  
V. G. Plotnichenko, S. L. Semjonov, and E. M. Dianov,  
Optics Express, v. 19, p. 1441 (2011)



# NCHCF – fiber design and loss spectrum

## Оптические свойства полых с дискретной симметрией границы сердцевина - оболочки



A. N. Kolyadin, A. F. Kosolapov, A. D. Pryamikov, A. S. Biriukov, V. G. Plotnichenko, and E. M. Dianov, Optics Express, v. 21, p. 9514 (2013)

# NCHCF – Optical losses spectrum in 2,5 – 8 mkm

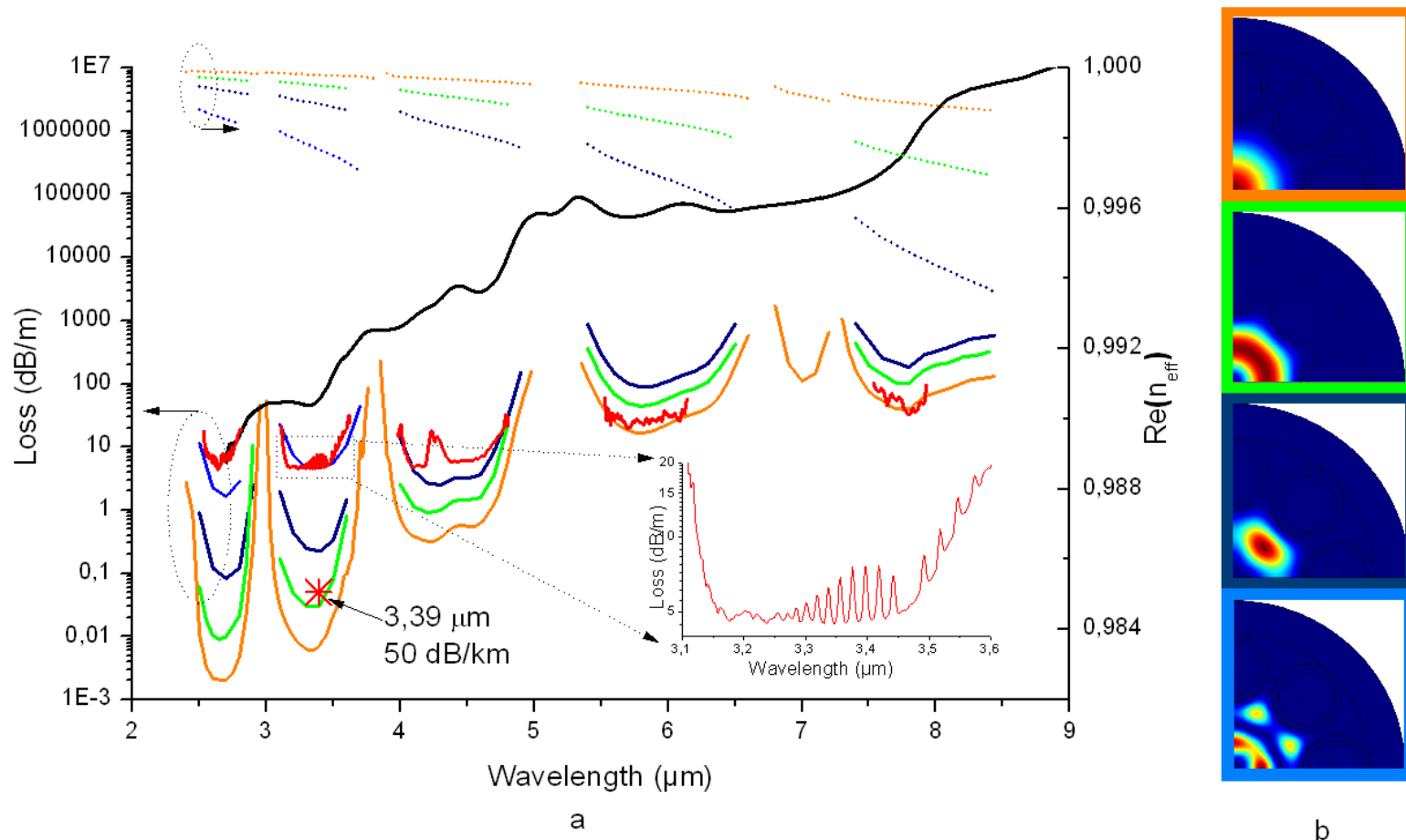
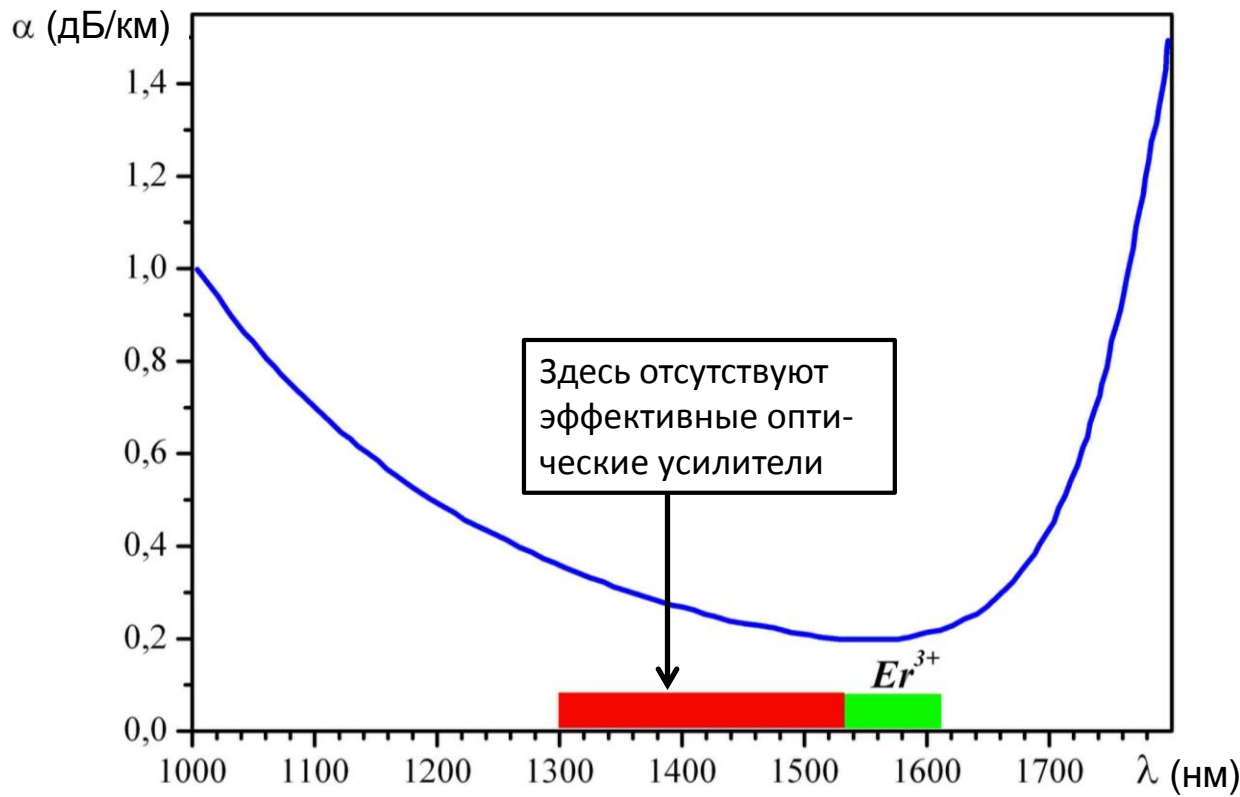


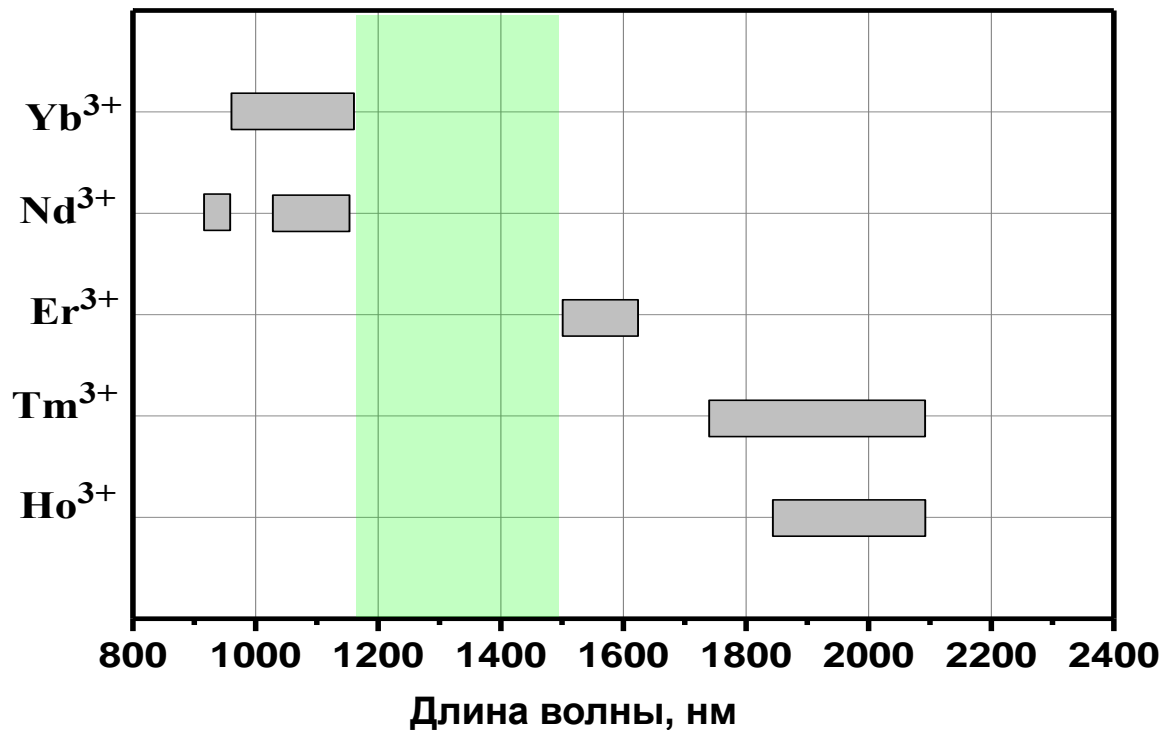
Fig. 2. a) The measured loss(Red); the loss measured with He-Ne at  $3.39 \mu\text{m}$ (red asterisk); the material loss in silica glass(black); the calculated loss (by left scale) and  $\text{Re}(n_{\text{eff}})$  (by right scale) of the fundamental mode(orange); the calculated loss (by left scale) and  $\text{Re}(n_{\text{eff}})$  (by right scale) of next higher order modes (green, navy, blue); b) the intensity distribution of the first several air core modes (color of frame corresponds to color of the line in the plot).

# Bismuth-doped fibers, lasers and amplifiers for 1000 ÷ 1700 nm

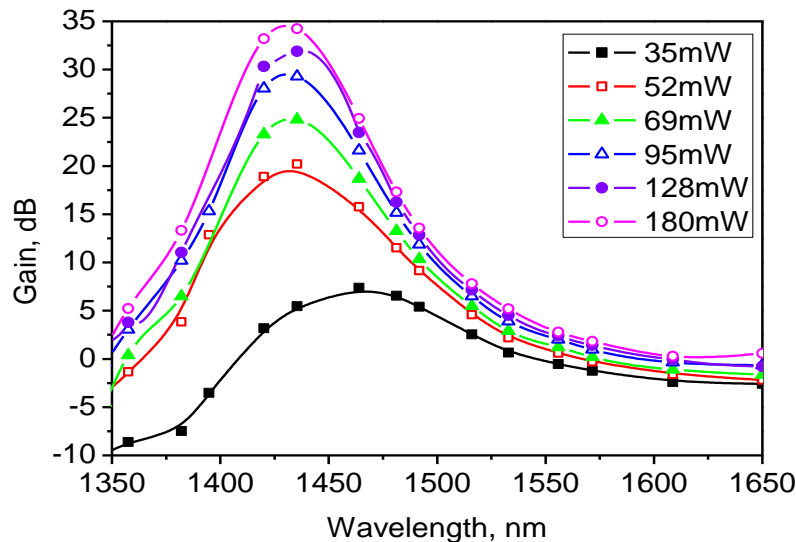
**Спектр минимальных оптических потерь волоконных  
световодов на основе кварцевого стекла**



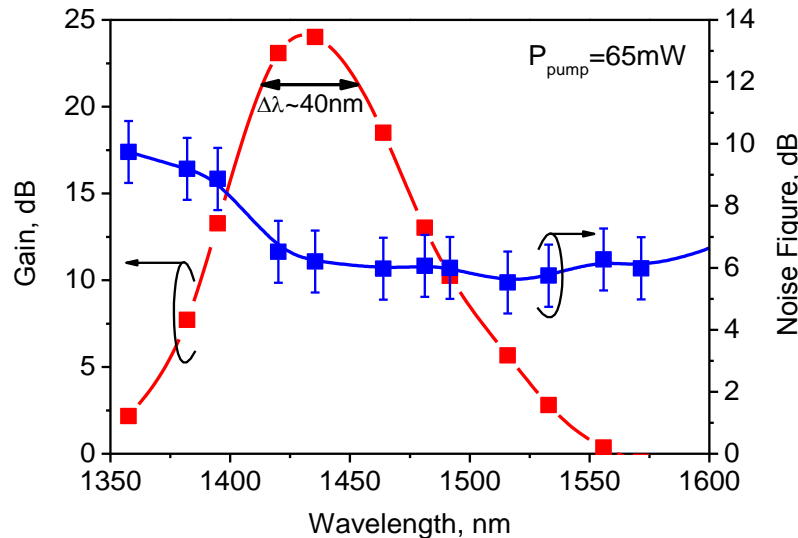
## Спектральные диапазоны эффективных волоконных лазеров на редкоземельных ионах



# Коэффициент усиления и шум-фактор висмутового волоконного усилителя, работающего на длине волны 1440 нм



Pump source – Raman fiber laser



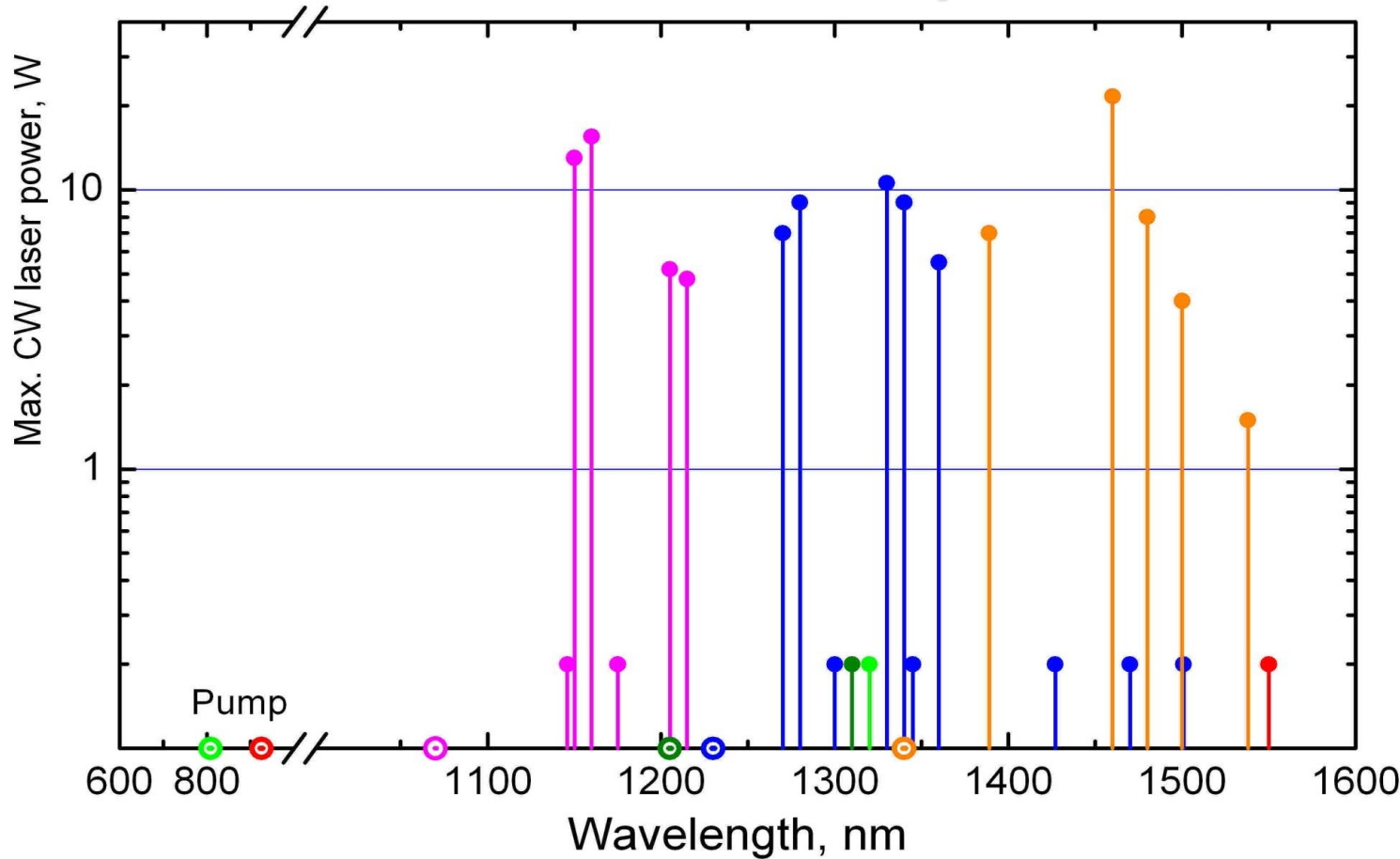
Pump source – laser diode  
 $P_{\text{pump}} = 65\text{mW}$  at 1310 nm

Peak net gain –  $G=35\text{dB}$  ( $P_{\text{pump}}=180\text{mW}$ )

Noise figure  $\sim 6\text{dB}$  ( $P_{\text{pump}}=65\text{mW}$ )

FWHM bandwidth –  $\lambda_{\text{FWHM}} \sim 40\text{nm}$  ( $P_{\text{pump}}=65\text{mW}$ )

# Диапазон длин волн генерации висмутовых волоконных лазеров



I.A.Bufetov, E.M.Dianov, Laser Physics Letters, 6, 487 (2009)  
M.A. Melkumov et al., Optics letters, 2012 (posted 4.05.2012)

# High-power, high-stable, single-frequency SC-FP+FBG lasers

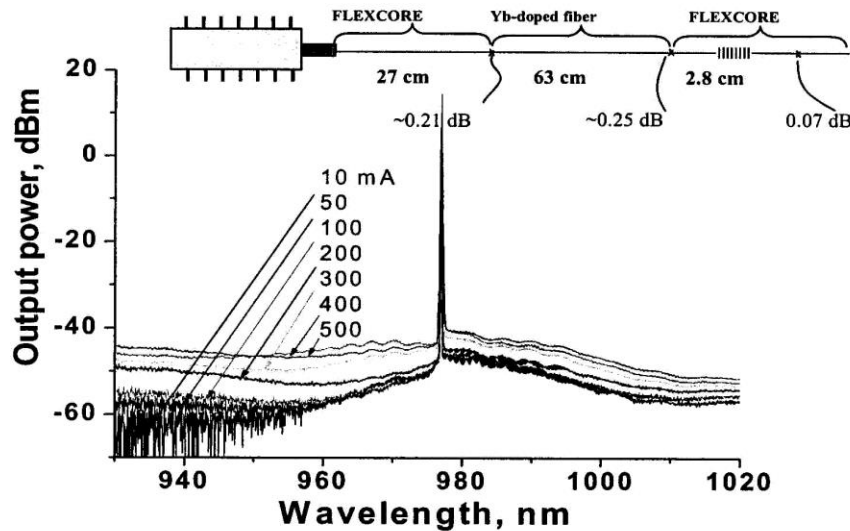


Fig. 3. SDL-2 spectra as a function of drive current with the Yb-doped fiber as an intra-cavity element. The inset shows the cavity design.

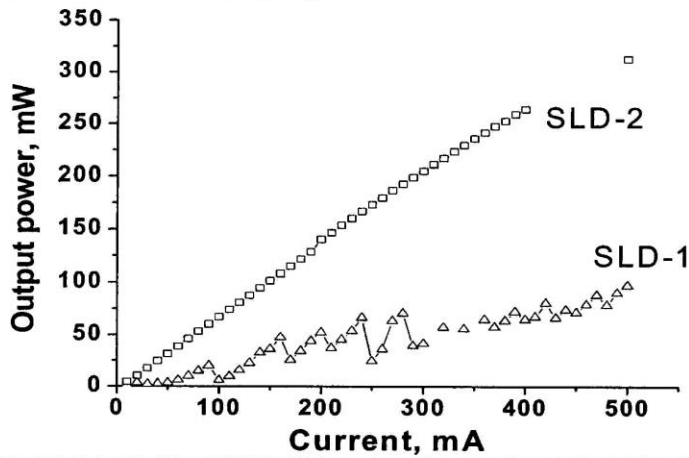


Fig. 4. L-I characteristics of SDL-2 with the cavity configuration shown in Fig. 3 (□), and for SLD-1 (Δ).

Table 1: Summary data on lasers with an external cavity used in experiments

Laser	SDL1	SDL2
Semiconductor chip FP mode spacing, nm	0.086	0.085
Doped fiber type	YbH	YbL
Doper Fiber length, cm	12.2	63
Doped fiber absorption bandwidth (FWHM), nm	~4	~1.9
Doped fiber absorption, dB/cm	3.3	0.23
FG bandwidth (FWHM), nm	0.21	0.2
FG reflectivity, %	75	80
Bragg wavelength, nm	976.55	976.6

Two cavities were fabricated for these experiments, each with similar Bragg grating, but different absorption and length of Yb doped fiber, as described in Table 1.

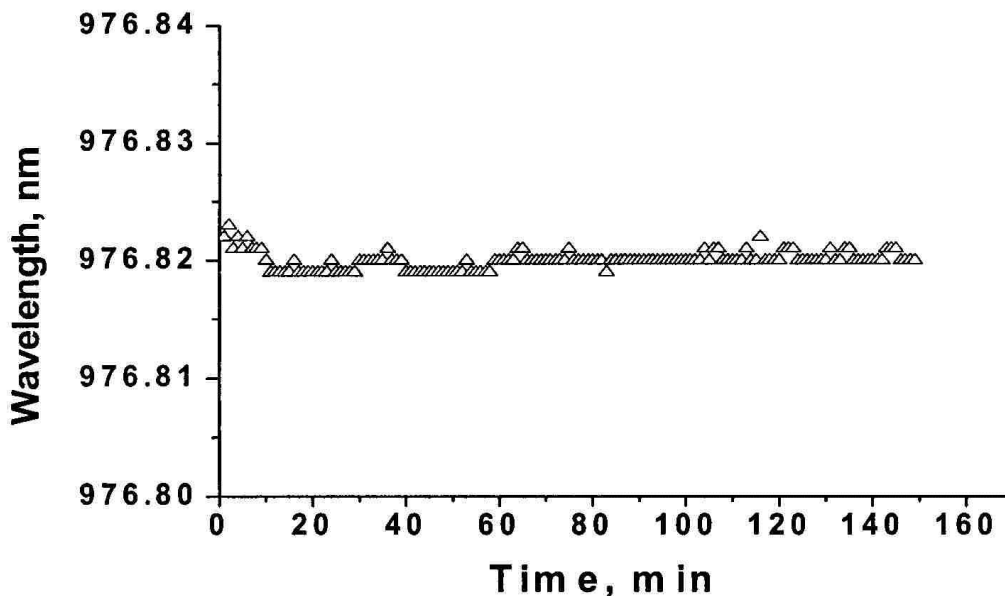


Fig. 6. Long term operating wavelength stability of SDL2 external resonator laser measured with a wavelength meter.

### 3.4. Broad-band tunable (~40 nm) single-frequency all-fiber DFB-lasers

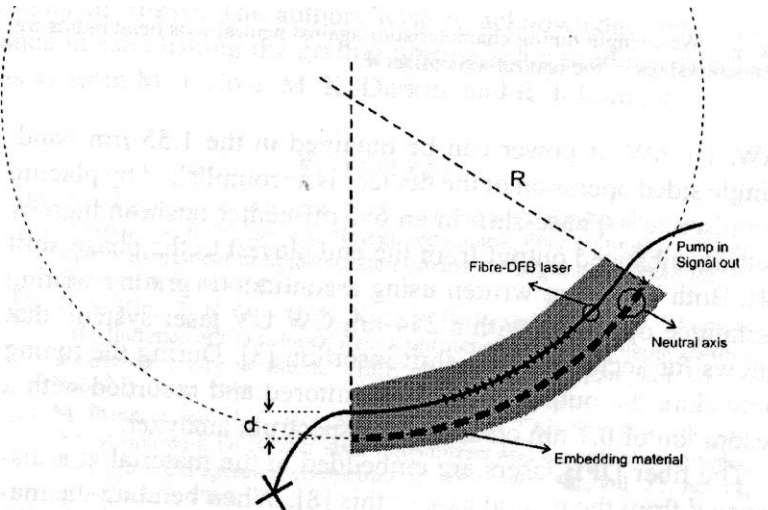


Fig. 1. Schematic principle of beam-tuning technique with indication of the bending arc radius  $R$  and the positioning  $d$  of the device under test relative to the neutral axis.

- A highly doped Er/Yb single-mode fiber
  - Two  $\pi$ -phase-shifted FBG – DFB fiber lasers, lengths of 4 and 5 cm
  - Pumping 976 nm, 70 mW
  - Stable output power 10 mW in the 1.55- $\mu\text{m}$  band
  - Tuning by bending the plate with fiber DFB laser - compression/extension of FBG
  - 27-nm continuous tuning ( 22.5-nm compression + 4.5-nm extension)
- The technique is reliable and simple

M.Ibsen, S.Y.Set, G.S.Goh, K.Kikuchi. **Broad-Band Continuously Tunable All-Fiber DFB Lasers.**  
– IEEE Photonics Technology Letters, Vol.14, No 1, 21-23 (2002).

## 27-nm continuous tuning characteristics of 4-cm-long fiber DFB-laser.

- Power stability in 1530 – 1550 nm range
- Tuning by compression is preferable

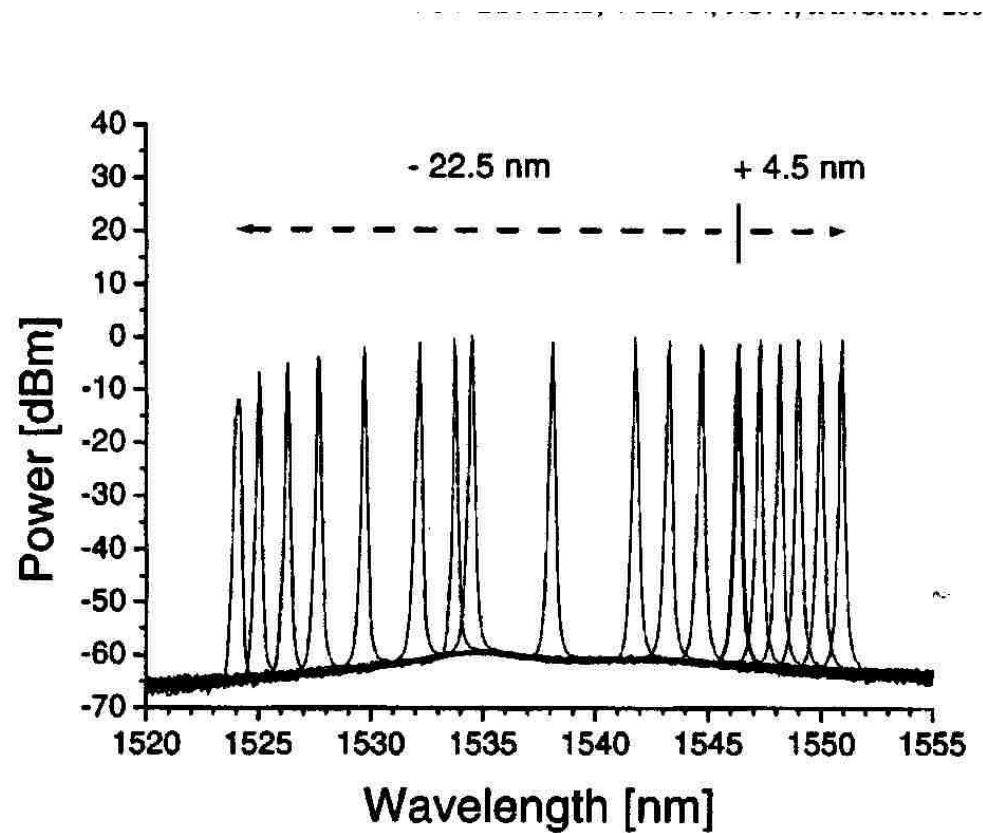


Fig. 3. 27-nm continuous tuning (22.5-nm compression + 4.5-nm extension) characteristics of 4-cm-long fiber DFB-laser.

# Wide Tunable Single-Mode Fiber Ring Laser

( $\Delta\lambda = 40 \text{ nm}$ ,  $\lambda = 1522 - 1562 \text{ nm}$ ,  $\Delta\nu \sim 750 \text{ Hz}$ )

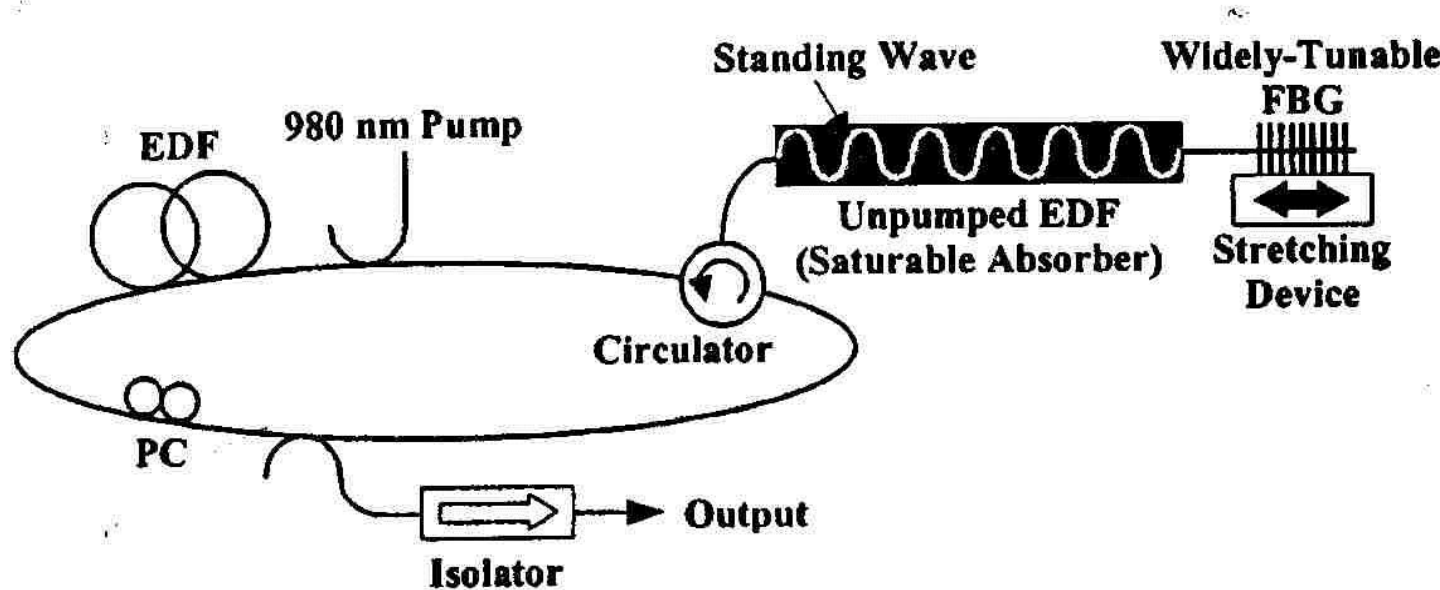


Fig. 1. Fiber ring laser configuration using a widely tunable FBG along with a saturable absorber to provide stable single-mode operation.

Y.S.Song, S.A.Havstad, D.Starodubov, Y.Xie, A.E.Willner, J.Feinberg. 40-nm-Wide Tunable Fiber Ring Laser With Single-Mode Operation Using a Highly Stretchable FBG. – IEEE PHOTONICS TECHNOLOGY LETTERS, Vol.13, NO. 11, pp.1167-1169, 2001.

# Continuous Tunable Fiber Ring Laser Operation Characteristics in 1520 – 1560 nm

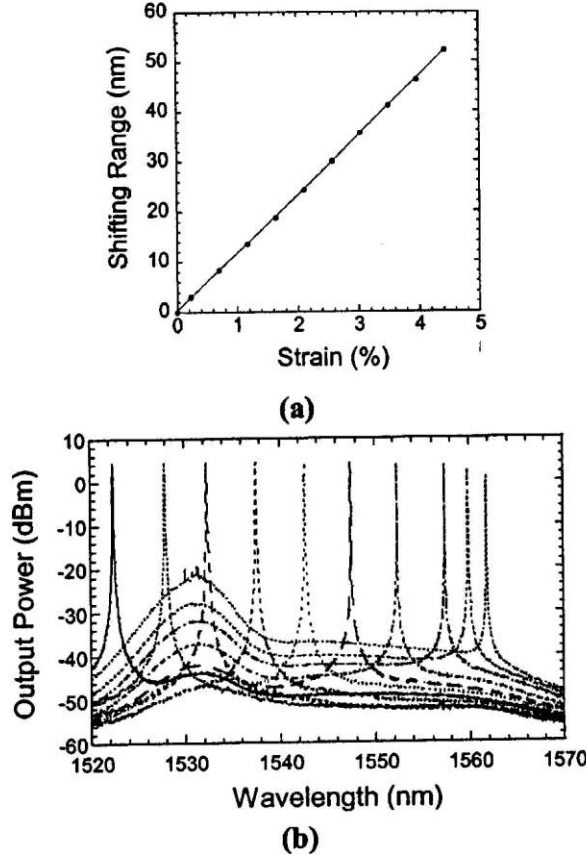


Fig. 2. (a) Measured tuning range of our widely tunable FBG. (b) Spectra of shifted laser output peaks with a 5% outcoupling fraction.

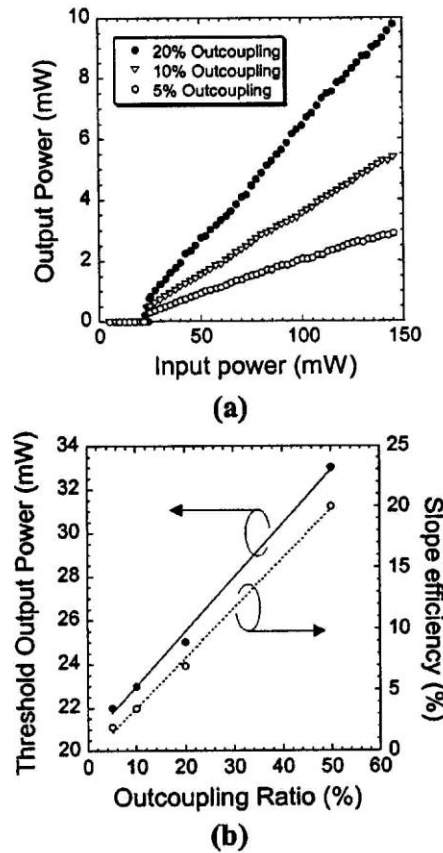


Fig. 3. (a) Lasing characteristics with various outcoupling ratios  
Threshold output power and slope efficiency variations with outcoupling ratio

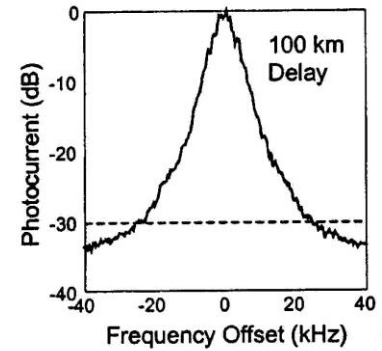


Fig. 5. Delayed self-heterodyne interferometer output power spectrum (100-km delay), indicating a linewidth of less than 1 kHz.

Linewidth  
 $\Delta\nu = 750 \text{ Hz}$

## Conclusion

This report reviews some recent achievements in fiber optics and fiber-coupled diode lasers, which can be useful for diode laser spectroscopy:

### New fibers

1. *Microstructured fibers have very large mode field diameters ~ 40 – 105 mkm.*
2. *Hollow-core PCF fibers are shown to be promising for in-line high sensitivity gas analysis.*
3. *New silica negative curvature hollow core fibers (NCHCF) can operate in spectral range 2,5 – 8 mkm.*

### New lasers

1. *New bismuth-doped fibers, lasers and amplifiers can operate in spectral range 1000 – 1700 nm.*
2. *Diode lasers with external cavity based on an active fiber (doped with Yb/Er) and an FBG can demonstrate a stable single frequency range of tunability wider than 40 nm and can be more advantageous for TDLS than DFB laser diodes.*

We are waiting for DFB fiber single frequency tunable lasers based on bismuth-doped fibers in spectral range of ~ 1400 – 1500 nm.